

RESEARCH

Open Access



# MYLK-AS1 improves fracture by targeting miR-146a-5p to regulate cell viability and apoptosis in osteoblasts

Wuluhan Mahan<sup>1†</sup>, Haoze Gao<sup>2†</sup>, Ning Liu<sup>3</sup>, Zhenyu Zhao<sup>3</sup> and Yingxuan Huang<sup>4,5\*</sup>

## Abstract

**Background** Delayed fracture healing (DFH) is a significant burden for patients. Therefore, early diagnosis and detection are important for the treatment of DFH. The long non-coding RNA (LncRNA) MYLK-AS1 is abnormally expressed in patients with DFH and has the potential to be used as a diagnostic marker.

**Methods** 40 patients with DFH and 87 patients with normal fracture healing were included. The levels of MYLK-AS1, miR-146a-5p and several mRNA markers of osteogenic differentiation were assessed by RT-qPCR. The diagnostic value of MYLK-AS1, miR-146a-5p was assessed using ROC curves. Cell proliferation ability was assessed by CCK-8, and apoptosis rate was detected by flow cytometry. DLR, RIP and RNA pull down assays demonstrated the targeting relationship between MYLK-AS1 and miR-146a-5p.

**Results** MYLK-AS1 levels were significantly lower and miR-146a-5p levels were significantly up-regulated in DFH compared to normal healing patients. MYLK-AS1 was found to target miR-146a-5p, and the levels were negatively correlated with each other. MYLK-AS1 with miR-146a-5p is of high value for the diagnosis of DFH. High expression of MYLK-AS1 could inhibit miR-146a-5p levels, support cell proliferation, reduce apoptosis, and increase the levels of osteogenesis-specific matrix proteins and osteogenesis-related regulatory factors.

**Conclusion** MYLK-AS1 has potential as a diagnostic marker for DFH. By increasing the expression level of MYLK-AS1 in cells can reduce the level of miR-146a-5p, increase the activity of osteoblasts and reduce their apoptosis rate, thus affecting the process of fracture healing.

**Keywords** MYLK-AS1, miR-146a-5p, Delayed fracture healing, Diagnostic marker

<sup>†</sup>Wuluhan Mahan and Haoze Gao contributed equally to this work.

\*Correspondence:

Yingxuan Huang  
gxhuangyx@163.com

<sup>1</sup>Department of Orthopedic Trauma, The First Affiliated Hospital of Xinjiang Medical University, Urumqi 830011, China

<sup>2</sup>The Third Clinical Medical College of Guangzhou University of Chinese Medicine, Guangzhou 510405, China

<sup>3</sup>Department of Orthopedics, The 2nd Affiliated Hospital of Harbin Medical University, Harbin 150086, China

<sup>4</sup>Guangxi Key Laboratory for Preclinical and Translational Research on Bone and Joint Degenerative Diseases, Baise 533000, China

<sup>5</sup>Pediatric Intensive Care Unit, The Affiliated Hospital of Youjiang Medical University for Nationalities, No. 18, Zhongshan 2nd Road, Youjiang District, 533000 Baise, China



## Background

Bone fractures are usually caused by a large external impact. Patients with fractures experience localized bone deformity and pain [1]. Fracture healing is an organ repair process that clinically involves osteogenesis, healing tissue formation, and remodeling [2]. The majority of fracture patients heal normally, but there are still 5–10% of fracture patients with slow fracture healing, delayed fracture healing (DFH), or even non-healing, causing pain to the patient and additional economic burden [3]. Early identification of fractures with signs of delayed healing can lead to earlier clinical intervention. Therefore, early diagnosis and detection are important in the management of DFH.

It has been reported that long non-coding RNAs (lncRNAs) have great potential to become diagnostic or prognostic biomarkers due to their aberrant expression in a variety of diseases [4, 5]. lncRNAs play an important role in many musculoskeletal diseases [6–11]. On the other hand, microRNAs (miRNAs) are also important regulators of various genes that contribute to the pathogenesis of disease [12], modulating cellular activity by targeting numerous signaling pathways or genes that promote or inhibit disease progression [13, 14]. Furthermore, given the important role of lncRNAs and miRNAs in regulating cell differentiation and the cell cycle, they represent a promising and viable source of biomarkers [15]. They could make an important contribution to the diagnosis of DFH status, the identification of drug targets, and the assessment of the efficacy of therapeutic interventions. In addition, lncRNAs can regulate the fracture healing process by influencing the physiological activities of osteoblasts (e.g. differentiation, proliferation, etc.) through various mechanisms [16].

The lncRNA MYLK antisense RNA 1 (MYLK-AS1), located on human chromosome 3q21.1, is 74,815 nt long and contains three exons [17]. Previous studies have reported that MYLK-AS1 has potential as a biomarker in a variety of diseases. These include colorectal cancer [18] and neuroblastoma [19]. In addition, the expression of MYLK-AS1 in bone marrow mesenchymal stem cells varies in different age groups, and the level of MYLK-AS1 in bone marrow mesenchymal stem cells of the elderly is significantly lower than that of adults, and the osteogenic derivation of bone marrow MSCs is an important part of fracture healing. Interestingly, Li et al. 2022 identified several differentially expressed lncRNAs by microarray in patients with normal healing and long-term non-healing fractures, in which MYLK-AS1 was significantly reduced [20]. In addition, miR-146a-5p was found to be significantly increased in tissues with non-healing fractures [21]. A study by Ren et al. also showed that miR-146a-5p can influence the osteogenic differentiation of periodontal ligament stem cells [22]. However, the potential role of

MYLK-AS1 and miR-146a-5p in fracture healing has not been reported. Based on the DIANA and lncRNASNP2 databases, which predicted a target relationship between the two, the present research was conducted to evaluate the diagnostic value of MYLK-AS1 and miR-146a-5p in fracture healing and their potential regulatory roles.

## Materials and methods

### Patient inclusion

40 patients with delayed fracture healing from May 2022 to February 2024 in The 2nd Affiliated Hospital of Harbin Medical University were included. 87 patients with normal fracture healing in the same period were included as a normal control group. Inclusion criteria: (a) All were first fractures and systematically treated; (b) both normal and delayed healing met the diagnostic criteria. Exclusion criteria: (a) with diabetes mellitus; (b) with osteoporosis or metabolic bone disease; (c) with other bone diseases. The clinical characteristics of the patients are shown in Table 1.

The study was approved by the Ethics Committee of the The 2nd Affiliated Hospital of Harbin Medical University Hospital. And in accordance with the Declaration of Helsinki, and the patients and their families signed an informed consent form.

### Cell culture and transfected

MC3T3-E1 cells were chosen for culture. The culture was performed using MEM- $\alpha$  medium containing nucleosides and GlutaMAX supplements as a blank group. MC3T3-E1 cells were cultured in ObM medium as the OM group. The medium contained 10% FBS (Gibco, USA) and was cultured at 37 °C with a CO<sub>2</sub> concentration of 5%.

MC3T3-E1 cells were inoculated at a density of  $3 \times 10^4$  cells/well and grown overnight in 6-well plates. The pcDNA3.1 empty vector and pcDNA3.1-MYLK-AS1 plasmid, miR NC with miR-146a-5p mimics were transfected into MC3T3-E1 cells by the Lipofectamine 3000 kit (Invitrogen, USA).

### RNA extraction

5 mL of fasting peripheral venous blood was collected from fracture patients at different stages of healing, and the serum was collected by centrifugation for 2 min. According to the volume of serum, 1 mL of Trizol reagent (Thermo Fisher, USA) was added and thoroughly mixed to completely lyse the cells and release the RNA, then 0.2 mL of chloroform was added and the cells were shocked for 15 s. The supernatant was collected by centrifugation at 12,000 g for 15 min at 4 °C. Centrifuge at 12,000 g for 15 min at room temperature and remove the supernatant. 0.5 mL isopropanol was added, mixed thoroughly and allowed to stand for 10 min, then centrifuged at 12,000 g

**Table 1** Clinical baseline characteristics of patients with normal and delayed healing

Parameters	Healing group (n = 87)	Delayed group (n = 40)	P value
Age, (year)	57.57±6.72	56.17±5.59	0.254
BMI, (kg/m <sup>2</sup> )	24.28±3.60	25.03±3.75	0.285
Gender, male, n (%)	41 (47.13)	20 (50.00)	0.849
Smoking history, n (%)	58 (66.67)	26 (65.00)	0.843
Drinking history, n (%)	53 (60.92)	23 (57.50)	0.952
Causes of fracture, n (%)			
Traffic accident	42 (48.28)	13 (32.50)	0.369
Falling from height	29 (33.33)	16 (40.00)	
Fall-related injury	9 (10.34)	7 (17.50)	
Blunt Trauma	7 (8.05)	4 (10.00)	
Fracture site, n (%)			
Upper limb	23 (26.44)	15 (37.50)	
Lower limb	33 (37.93)	18 (45.00)	0.107
Spine	31 (35.63)	7 (17.50)	
Classification of fracture, n (%)			
Closed fracture	35 (40.23)	16 (40.00)	0.980
Open fracture	52 (59.77)	24 (60.00)	
AO classification of fracture, n (%)			
A	33 (37.93)	10 (25.00)	0.083
B	46 (52.87)	21 (52.50)	
C	8 (9.20)	9 (22.50)	
ASA Classification, n (%)			
II	67 (77.01)	18 (45.00)	0.001
III-IV	20 (22.99)	22 (55.00)	

Annotation: BMI, body mass index. AO, Arbeitsgemeinschaft für Osteosynthesefragen; ASA, American Society of Anesthesiologists

for 10 min at 4 °C and the supernatant discarded. The precipitate was washed with 1 mL of 75% ethanol, vortexed and mixed well, centrifuged at 7500 g for 5 min at 4 °C and the supernatant discarded. The precipitate was dried and dissolved in RNase-free water to obtain total RNA.

#### RT-qPCR

1 µL of Oligo (dT) was added according to the volume of RNA, filled up to 12 µL with RNase-free water, mixed and reacted at 65 °C for 5 min on the PCR instrument to allow primer binding. Then 4 µL 5× reaction buffer, 1 µL Ribolock RNase inhibitor, 2 µL 10 mM dNTP mix and 1 µL RevertAid m-mul URT were added. 20 µL of total system was added. The PCR instrument was set at 42 °C for 1 h, 70 °C for 5 min and terminated at 4 °C. RNA purity was determined and OD260:OD280 was in the range of 1.7–2.1. Specific primers were then designed using Primer5.0 software, and the primer sequences, registration numbers and T<sub>m</sub> temperatures of the genes are shown in Table S1. cDNA obtained from reverse transcription was used as a template for PCR amplification. First, the reaction system was configured, including 2 µL cDNA template, 10 µL 2×SYBR Green qPCR Mix, 0.4 µL each of 10 µM primer forward and 10 µM primer reverse, and 7.2 µL nuclease-free water. The PCR amplification cycle was programmed as follows: pre-denaturation,

95 °C for 300 s, denaturation 95 °C for 20 s, and denaturation 95 °C for 20 s. The reaction system was set up as follows: 300 s, denaturation 95 °C for 20 s, annealing 55 °C for 20 s, and extension 72 °C for 20 s. Forty cycles were performed. At the end of the amplification cycle, the temperature was lowered to 60 °C and then heated to 95 °C to denature the DNA product. All sample sets showed significant fluorescence signals characterized by smooth and ordered amplification curves and a single peak in the melting curve. This indicates the absence of primer dimerization and confirms that this is consistent with the required amplification efficiency. GAPDH and U6 were used as endogenous references. Assay results were normalized by the 2<sup>-ΔΔCT</sup> method. Differences in Ct values ((ΔDelta Ct) of MYLK-AS1 and GAPDH or miR-146a-5p and U6 were calculated to determine the relative RNA levels, as follows formula: ΔΔ Ct = (Δ Ct of the patient sample)– (Δ Ct of the control sample).

#### Cell viability assay

The proliferative capacity of the cells was assessed using the CCK-8. Briefly, 200 µL of cell suspension was seeded into a 96-well plate, with three replicate wells per group. Then, 200 µL of PBS was added around the cell-containing wells to form a circular border. The cells were incubated for 24 h, after which 10 µL of CCK-8 solution was

added to each well. After a further 1 h incubation, the absorbance at 450 nm (OD450) was measured by shaking the plate for 30 s on an enzyme plate reader.

#### Cell apoptosis assay

MC3T3-E1 cells were harvested at a density of  $2 \times 10^4$  cells/mL. After three washes with PBS, the cells were collected by centrifugation (1000 rpm, 5 min) and the supernatant was discarded. To the resulting pellet, 100  $\mu$ L binding buffer was added. Then, 5  $\mu$ L PI and Annexin V-fluorescein isothiocyanate were added, and the cells were incubated in the dark for 15 min. After incubation, 300  $\mu$ L of 1 $\times$  binding buffer was added to the mixture. Finally, the suspension was transferred to a flow cytometry tube and analysed by flow cytometry under light avoidance conditions.

#### Alkaline phosphatase (ALP) activity assay

Cells were first fixed with 4% paraformaldehyde in PBS (pH 7.4) and then washed with PBS. Finally, ALP activity was assessed using the ALP activity kit (Beyotime, Shanghai).

#### Bioinformatics analysis

The binding site of MYLK-AS1 to miR-146a-5p was predicted by DIANA (<https://diana.e-ce.uth.gr/lncbasev3>) and LncRNASNP2 (<https://guolab.wchscu.cn/lncRNASNP/#/>) databases.

#### Dual-luciferase reporter assay (DLR) assay

Wild-type recombinant MYLK-AS1 (MYLK-AS1-WT) and mutant recombinant MYLK-AS1 (MYLK-AS1-MUT) plasmids were constructed using the pmirGLO vector. The recombinant plasmids were co-transfected with miR-146a-5p blank or mimic group using Lipofectamine 3000 kit (Invitrogen, USA) and detected using DLR kit (Beyotime, Shanghai).

#### RIP assay

The RIP assay was used to detect the binding of RNA to proteins. Cells were resuspended with a volume of RIP lysate equal to that of the cells and then incubated with antibody-coupled magnetic beads at 4°C overnight. After washing, RNA was purified and reverse transcribed into cDNA according to the assay procedure of RT-qPCR to detect the level of the target.

#### RNA pull-down assay

Biomarker-labelled RNA (Bio-NC-probe, Bio-MYLK-AS1-probe) was used to treat MC3T3-E1 cells. Lysis was performed by adding lysate, and streptavidin magnetic beads (Thermo Fisher, USA) were added to the lysate and incubated at 4°C overnight. The magnetic beads were separated by centrifugation and the supernatant was

collected. The enrichment of miR-146a-5p in the supernatant was assessed by RT-qPCR.

#### Statistical analysis

Data are presented as mean  $\pm$  SD. All tests were performed at least 3 times with parallel testing. Patients' clinical data were collected and tabulated using SPSS, and the remaining data were collected and plotted using GraphPad. ROC curve evaluation was used to determine the diagnostic role of MYLK-AS1 and miR-146a-5p. A *p*-value of below 0.05 indicates that the difference between the two groups is statistically significant.

## Results

### Expression of MYLK-AS1 and miR-146a-5p

During the healing period of fracture patients, the expression level of MYLK-AS1 was significantly reduced in patients with DFH compared to patients with normal healing ( $P < 0.0001$ , Fig. 1A), while miR-146a-5p levels were significantly upregulated in patients with delayed healing during the 1–12-week healing cycle ( $P < 0.0001$ , Fig. 1B). Moreover, the clinical data of the two groups of patients were compared and it was found that there was no significant difference between the two groups in terms of age, BMI, smoking history, drinking history, causes of fracture, fracture site, fracture classification, AO classification of fracture ( $P > 0.05$ ). However, there was a significant difference in ASA classification ( $P = 0.001$ , Table 1).

### Diagnostic value of MYLK-AS1 and miR-146a-5p

The diagnostic performance of MYLK-AS1 versus miR-146a-5p for DFH was predicted by ROC curves. The ROC curve for MYLK-AS1 had an AUC of 0.853 (95% CI 0.783–0.923), a sensitivity of 72.5%, and a specificity of 82.76% for discriminating patients with delayed healing from the normal healing group (Fig. 1C). The AUC for miR-146a-5p was 0.826 (95% CI 0.748–0.903), with a sensitivity of 67.50% and a specificity of 87.36% (Fig. 1D). In addition, the results of binary logistic analyses showed that ASA classification, MYLK-AS1, and miR-146a-5p were factors influencing delayed fracture healing (Table 2).

### Effect of induction of osteogenic differentiation on osteogenic gene

As illustrated in Fig. 2, OM promoted osteoblast differentiation and ALP activity, and the expression levels of Runx2, BMP2, OCN, OPN, and MYLK-AS1 in cells cultured in the OM group were significantly higher than those in the blank control group from the third day of culture ( $P < 0.001$ , Fig. 2A–F). With increasing days of culture, the difference between the blank group and the OM groups increased. Compared to the blank group, miR-146a-5p was decreased in the OM group ( $P < 0.001$ ), and

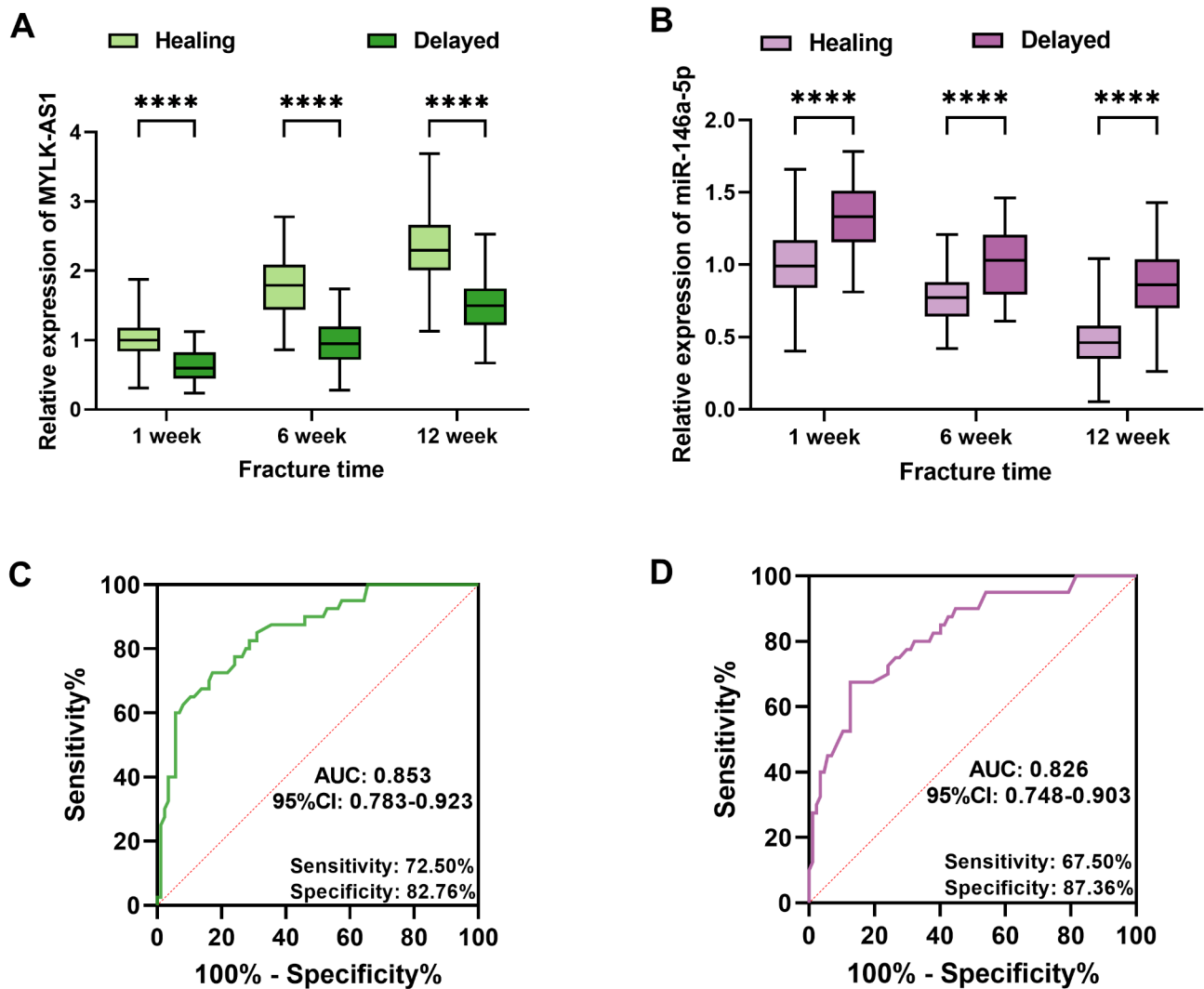


**Fig. 1** Expression and diagnostic roles of MYLK-AS1 and miR-146a-5p. **A** MYLK-AS1 is lowly expressed in patients with DFH; **B** miR-146a-5p was highly level in patients with delayed fracture healing; **C** and **D** MYLK-AS1 and miR-146a-5p have a better diagnostic role in distinguishing patients with normal healing from those with DFH (\*\*\*\*  $P < 0.0001$ )

**Table 2** Binary logistic regression analysis affecting delayed healing in fracture patients

Parameters	B	Wald	OR	95% CI	P value
Age	0.711	1.588	2.037	0.674 - 6.160	0.208
BMI	-0.237	0.207	0.789	0.285 - 2.187	0.649
Male	-0.465	0.756	0.628	0.220 - 1.792	0.384
Smoking history	0.461	0.709	1.586	0.542 - 4.643	0.400
Drinking history	0.143	0.072	1.154	0.405 - 3.286	0.789
Traffic accident	0.690	1.675	1.993	0.701 - 5.663	0.196
Lower limb	0.356	0.381	1.428	0.461 - 4.422	0.537
Open fracture	0.133	0.061	1.143	0.397 - 3.288	0.805
AO classification of fracture	0.396	0.455	1.486	0.471 - 4.690	0.500
ASA Classification	1.869	10.713	6.483	2.117 - 19.854	<b>0.001</b>
MYLK-AS1	2.143	15.075	8.528	2.890 - 25.163	<b>0.000</b>
miR-146a-5p	-1.489	7.979	0.226	0.080 - 0.634	<b>0.005</b>

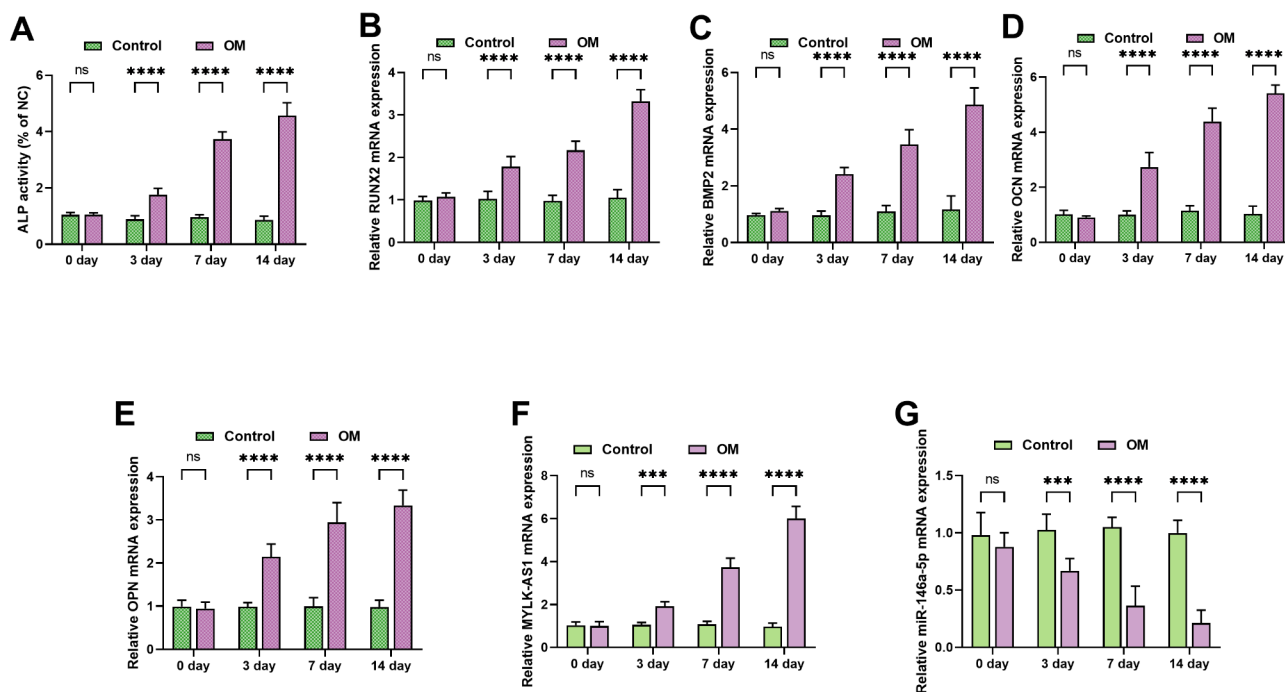


**Fig. 2** Difference between normal culture and OM medium culture of MC3T3-E1 cells. **A B** and **C** ALP, Runx2 and BMP2 levels of cells in OM medium were significantly increased within 14 days of culture; **D** and **E** OCN and OPN levels of cells in OM medium were significantly increased within 14 days of culture; **F** MYLK-AS1 levels of cells in OM medium were significantly increased within 14 days of culture; **G** miR-146a-5p levels of cells in OM medium were significantly increased within 14 days of culture (\*\* $P < 0.001$ , \*\*\*\* $P < 0.0001$ )

the decrease was more pronounced with increasing culture time ( $P < 0.0001$ , Fig. 2G).

#### Effect of MYLK-AS1 expression on cell function

Transfection of pcDNA3.1-MYLK-AS1 induced high levels of MYLK-AS1 in the cells ( $P < 0.0001$ , Fig. 3A). Increasing the level of MYLK-AS1 increased cell proliferation ( $P < 0.0001$ , Fig. 3B) and significantly decreased apoptosis ( $P < 0.0001$ , Fig. 3C). In addition, the activity of ALP, and the expression levels of Runx2, BMP2, OCN and OPN were also significantly upregulated when MYLK-AS1 was highly expressed (Fig. 3D and H).

#### MYLK-AS1 binds to miR-146a-5p targeting

MYLK-AS1 was predominantly enriched in the cytoplasm rather than in the nucleus (Fig. 4A). miR-146a-5p binding sites with MYLK-AS1-WT are shown in Fig. 4B. Targeted binding of miR-146a-5p and MYLK-AS1-WT was confirmed by DLR experiments. Transfection of miR-146a-5p mimics significantly reduced the luciferase activity of MYLK-AS1-WT ( $P < 0.01$ , Fig. 4C). Both miR-146a-5p and MYLK-AS1 were enriched in the anti-Ago2 group compared to the anti-IgG group (Fig. 4D). Compared to the bio-NC probe, miR-146a-5p was mainly enriched on the bio-MYLK-AS1-probe, which also indicated the binding relationship between miR-146a-5p and MYLK-AS1 (Fig. 4E). According to Pearson correlation analysis, miR-146a-5p showed an inverse correlation

with the MYLK-AS1 level ( $r = -0.755$ , Fig. 4F). Furthermore, miR-146a-5p levels were significantly decreased after transfection of pcDNA3.1-MYLK-AS1 ( $P < 0.0001$ , Fig. 4G).

#### Effects of MYLK-AS1 and miR-146a-5p on cellular

Transfection of pcDNA3.1-MYLK-AS1 resulted in an increase in the level of MYLK-AS1 and a significant decrease in the level of miR-146a-5p; whereas transfection of the miR-146a-5p mimic did not affect the level of MYLK-AS1, but only increased the level of miR-146a-5p ( $P < 0.0001$ , Fig. 5A and B). This suggests that miR-146a-5p is regulated by the level of MYLK-AS1. Increasing the level of MYLK-AS1 and decreasing the level of miR-146a-5p promoted cell proliferation decreased apoptosis, and increased ALP activity, the levels of Runx2, BMP2, OCN, and OPN mRNA ( $P < 0.0001$ ). However, increasing miR-146a-5p expression reversed this effect ( $P < 0.01$ , Fig. 5C and I).

#### Discussion

Fractures are usually treated clinically with surgery. However, the blood flow after fracture is poor and the post-operative prognosis often delays recovery. Moreover, the recovery period has many influencing factors and takes a long time, which greatly affects the patient's life, and creates a serious economic burden for the patient [23]. Delayed healing also increases the risk of secondary

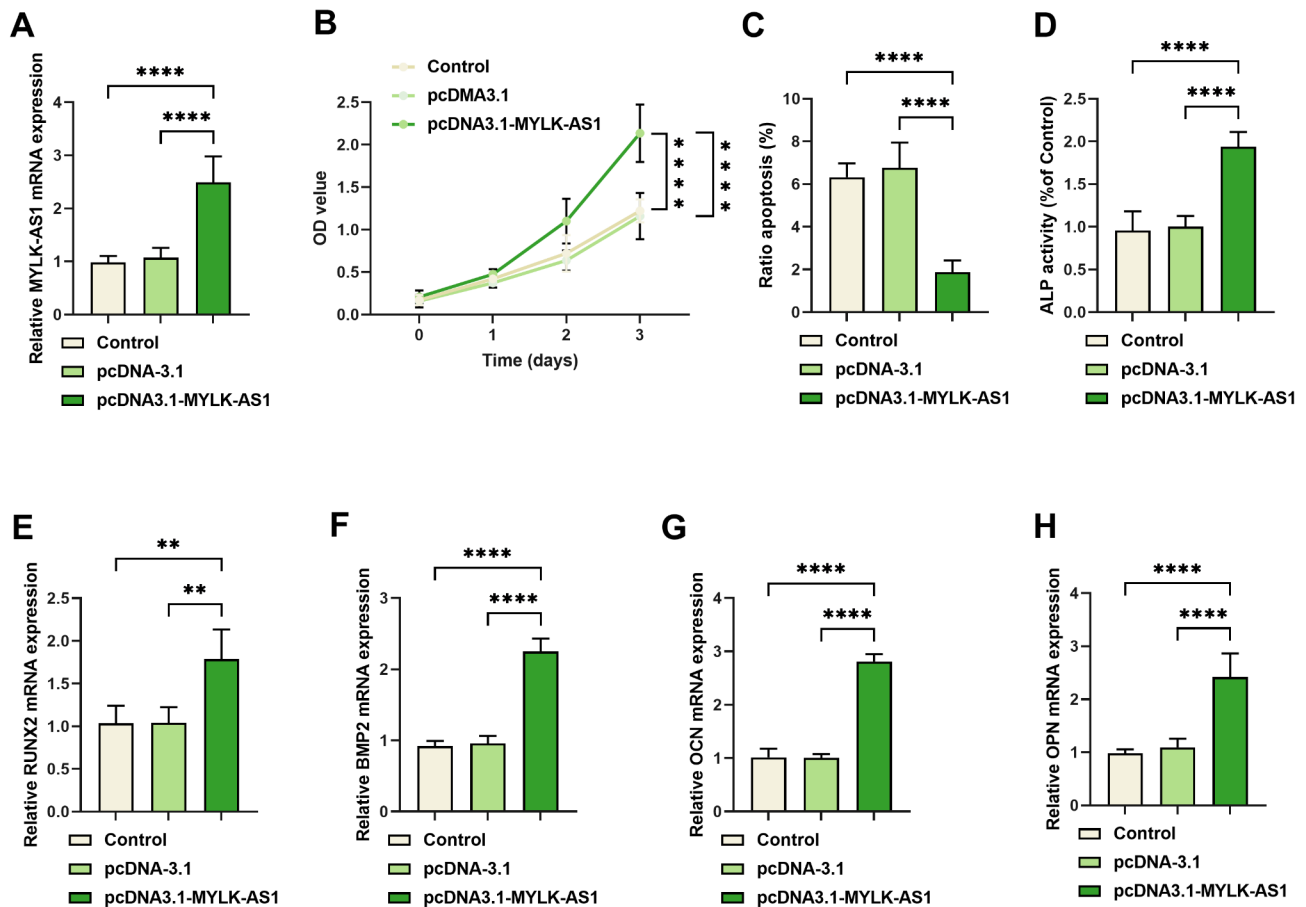


**Fig. 3** Effect of high MYLK-AS1 expression on fracture healing. **A** Transfection of MYLK-AS1 promotes its high expression; **B** High expression of MYLK-AS1 promotes cell proliferation; **C** High expression of MYLK-AS1 reduces apoptosis; **D** and **F** High expression of MYLK-AS1 notably increased the levels of ALP, RUNX2, BMP2; **G** and **H** High expression of MYLK-AS1 notably increased the levels of OCN and OPN (\*\*  $P < 0.01$ , \*\*\*\*  $P < 0.0001$ )

surgery and has a poor prognosis. Therefore, early detection of delayed fracture healing is important to improve patient patients [24]. It has been reported that lncRNAs can regulate post-transcriptional gene levels, are involved in a variety of physiological processes, and are potential predictive or diagnostic biomarkers for many diseases [25, 26].

In recent years, lncRNAs have been identified as key regulators in the complex process of fracture healing, such as TRPM2-AS [27] and SNHG1 [28]. Furthermore, lncRNAs act as sponges for miRNAs and may be involved in the disease process by regulating miRNAs [29]. There is evidence that miR-146a-5p is significantly increased in the tissues of rats with bone non-healing [21]. Our study showed the same trend, with miR-146a-5p being highly expressed during the recovery period in patients with delayed fracture healing. However, we also found that the lncRNA MYLK-AS1 was low expressed during the recovery period of fracture patients. ROC results showed that both MYLK-AS1 and miR-146a-5p have a better diagnostic role. It can discriminate between normal healing and delayed healing. It has a high diagnostic and predictive

value, suggesting that it may be involved in the pathological process of DFH.

Although the molecular mechanisms underlying the occurrence of delayed fracture healing are still unclear, an in-depth study of fracture healing at the cellular level may provide better diagnostic and therapeutic tools for delayed fracture healing. lncRNAs can regulate many physiological activities of osteoblasts, including cell migration, differentiation, proliferation, and apoptosis [30]. Cell differentiation and proliferation help to accelerate bone formation [31]. Further findings showed that increasing MYLK-AS1 levels significantly increased cell proliferation and decreased the rate of apoptosis. In addition, fluid shear stress was reported to downregulate downregulated miR-146a-5p levels in osteoblasts and inhibit osteoblast apoptosis [32]. Consistent with this study, we found that upregulation of miR-146a-5p promoted osteoblast apoptosis. This suggests that MYLK-AS1 is present in fracture healing as a factor that promotes fracture healing, whereas miR-146a-5p inhibits fracture healing.

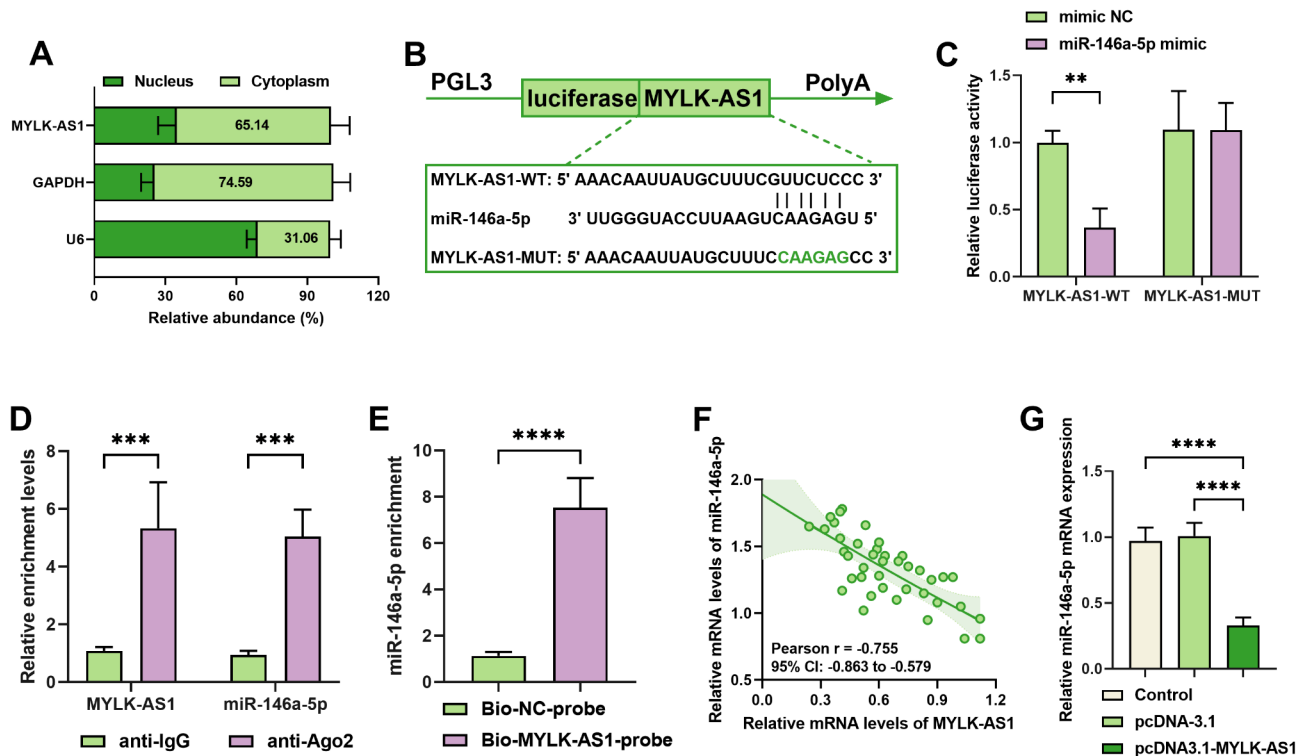


**Fig. 4** Targeted binding of MYLK-AS1 to miR-146a-5p. **A** MYLK-AS1 is mainly enriched in cytoplasmic; **B** Predicted binding site of MYLK-AS1 to miR-146a-5p; **C** miR-146a-5p mimic causes reduced luciferase activity in MYLK-AS1-WT; **D** Both miR-146a-5p and MYLK-AS1 were predominantly enriched in anti-Ago-2; **E** miR-146a-5p is predominantly enriched in Bio-MYLK-AS1-probe; **F** miR-146a-5p shows a typical negative correlation with MYLK-AS1 expression; **G** High expression of MYLK-AS1 leads to reduced miR-146a-5p levels (\*\*\* $P < 0.001$ , \*\*\*\* $P < 0.0001$ )

Osteoblast differentiation is important in bone recovery [33–36]. Osteogenesis-specific matrix proteins and osteogenesis-related regulators play important roles in fracture healing. Alkaline phosphatase (ALP), osteocalcin (OCN), and osteoblastin (OPN) all belong to the osteogenesis-specific matrix proteins [37, 38]. The main role of ALP is to hydrolyze phosphate esters during osteogenesis, releasing the inhibition of phosphate on bone salt formation, promoting osteoblasts proliferation and differentiation, and is an indicator of the activation response to osteogenic activation [39]. OCN is often used as a serum marker for bone formation in osteoblasts [40]. OPN can be involved in the regulation of the biological activities of bone-associated cells, such as proliferation, migration, and adhesion [41]. Therefore, in our study, when MC3T3-E1 cells were cultured using OM medium, the activity of ALP, the levels of OCN, and OPN were significantly increased, which promoted osteogenic differentiation of MC3T3-E1 cells. The same trend was observed when the expression level of MYLK-AS1 was increased. There was an improvement in the osteogenic differentiation capacity of the cells.

Runt-related transcription factor 2 (Runx2) and bone morphogenetic protein-2 (BMP-2) are key regulators of osteoblast differentiation and bone formation, respectively [42]. Endogenous BMP2 expression in

chondrocytes may play an important role in the maturation of cartilage healing tissue during the early stages of fracture healing [43]. Our results show that high levels of MYLK-AS1 promote elevated expression levels of Runx2 and BMP-2, which is reversed by high levels of miR-146a-5p. This suggests that miR-146a-5p exists as a detrimental factor in the fracture healing process. Increasing the level of MYLK-AS1 could reduce the expression of miR-146a-5p, which could affect the rate of fracture healing. However, more experiments are needed in this study to validate the existing results.

## Conclusions

In conclusion, high expression of MYLK-AS1 may contribute to fracture healing and has a better diagnostic value. Elevated levels of MYLK-AS1 lead to lower levels of miR-146a-5p, which promotes cell proliferation, osteogenic differentiation, and reduces apoptosis, thereby facilitating the process of fracture healing.

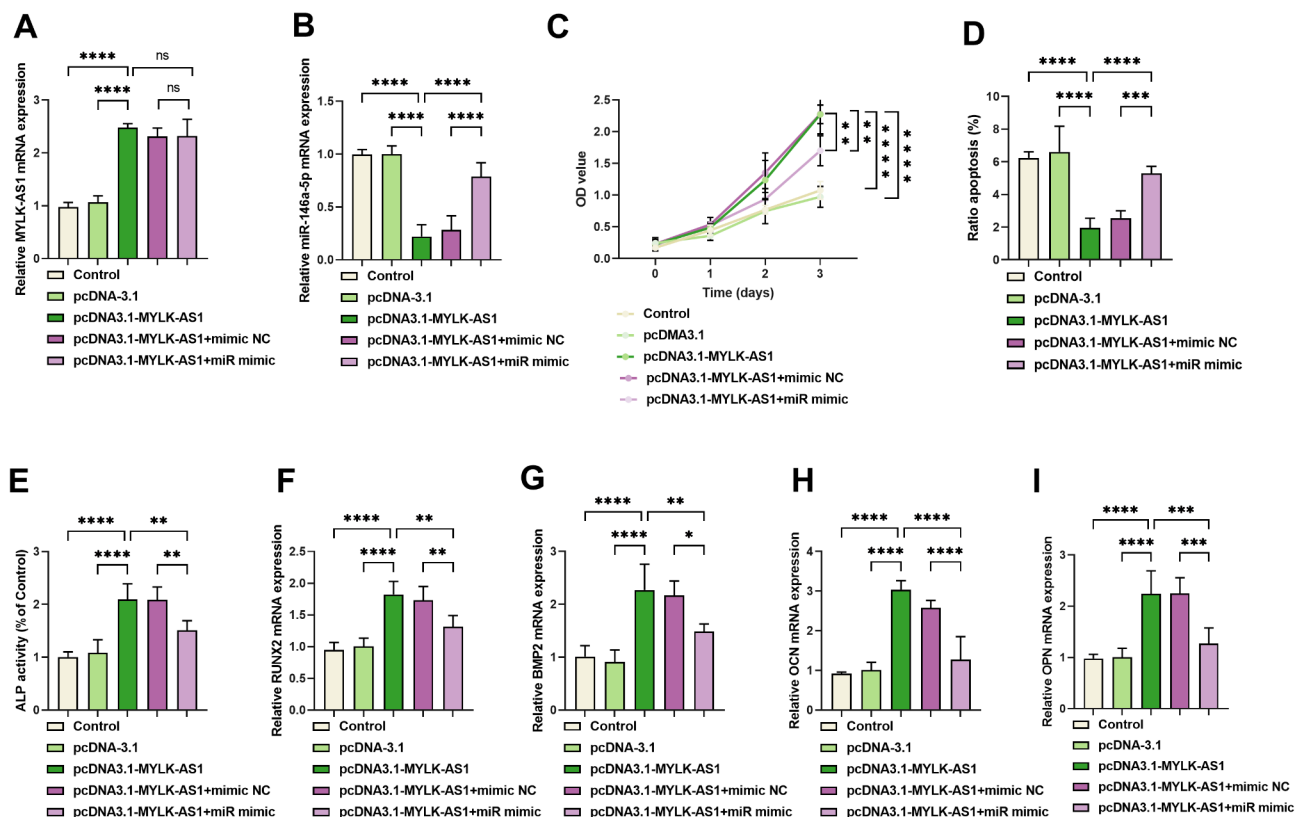


**Fig. 5** MYLK-AS1 and miR-146a-5p together affect fracture healing. **A** and **B** Transfection of MYLK-AS1 resulted in increased levels of MYLK-AS1 and a significant decrease in miR-146a-5p levels; whereas, transfection of miR-146a-5p mimic did not affect the levels of MYLK-AS1; **C** Increasing the level of MYLK-AS1 promotes cell proliferation, while increasing miR-146a-5p expression reverses the effect; **D** Increasing the level of MYLK-AS1 reduced apoptosis, while increasing the expression of miR-146a-5p reversed the effect; **E F** and **G** Increasing the level of MYLK-AS1 promotes the expression of ALP, RUNX2, and BMP2, which is reversed by increasing miR-146a-5p expression; **H** and **I** Increasing the level of MYLK-AS1 promotes OCN, OPN expression, which is reversed by increasing miR-146a-5p expression (\*\*  $P < 0.01$ , \*\*\*  $P < 0.001$ , \*\*\*\*  $P < 0.0001$ )

## Supplementary Information

The online version contains supplementary material available at <https://doi.org/10.1186/s13018-025-05688-1>.

Supplementary Material 1

## Acknowledgements

Not Applicable.

## Author contributions

NL and ZYZ conceived and designed the experiments. NL and ZYZ performed the experiments and contributed sample collection and statistical analysis. NL and ZYZ wrote the manuscript. WLH, MH, HZ, G and YX, H revised it critically for important intellectual content. All authors read and approved the final manuscript.

## Funding

No funding was received to assist with the preparation of this work.

## Data availability

The datasets used and/or analyzed during the current study are available from the corresponding author on reasonable request.

## Declarations

### Ethics approval and consent to participate

The study was performed in line with the principles of the Declaration of Helsinki. Approval was granted by the Ethics Committee of The 2nd Affiliated Hospital of Harbin Medical University before the study began. The written informed consent has been obtained from the participants involved.

### Consent for publication

Not applicable.

### Competing interests

The authors declare no competing interests.

### Conflict of interest

The author has no conflicts of interest to declare.

Received: 14 January 2025 / Accepted: 6 March 2025

Published online: 19 March 2025

## References

- Fernandes JB, Ferreira N, Domingos J, Ferreira R, Amador C, Pardo N et al. Health Professionals' Motivational Strategies to Enhance Adherence in the Rehabilitation of People with Lower Limb Fractures: Scoping Review. *Int J Environ Res Public Health*. 2023;20(22).
- Chacon EL, Bertolo MRV, de Guzzi Plepis AM, da, Conceição Amaro Martins V, Dos Santos GR, Pinto CAL et al. Collagen-chitosan-hydroxyapatite

- composite scaffolds for bone repair in ovariectomized rats. *Scientific reports*. 2023;13(1):28.
3. Jayankura M, Schulz AP, Delahaut O, Witvrouw R, Seefried L, Berg BV, et al. Percutaneous administration of allogeneic bone-forming cells for the treatment of delayed unions of fractures: a pilot study. *Stem Cell Res Ther*. 2021;12(1):363.
  4. Lu Q, Guo Q, Xin M, Lim C, Camero AM, Gerhard GS et al. LncRNA TP53TG1 promotes the growth and migration of hepatocellular carcinoma cells via activation of ERK signaling. *Non-coding RNA*. 2021;7(3).
  5. Zuo Y, Xiong C, Gan X, Xie W, Yan X, Chen Y, et al. LncRNA HAGLR Silencing inhibits IL-1 $\beta$ -induced chondrocytes inflammatory injury via miR-130a-3p/JAK1 axis. *J Orthop Surg Res*. 2023;18(1):203.
  6. Giordano L, Porta GD, Peretti GM, Maffulli N. Therapeutic potential of MicroRNA in tendon injuries. *Br Med Bull*. 2020;133(1):79–94.
  7. Oliviero A, Della Porta G, Peretti GM, Maffulli N. MicroRNA in osteoarthritis: physiopathology, diagnosis and therapeutic challenge. *Br Med Bull*. 2019;130(1):137–47.
  8. Gargano G, Oliviero A, Oliva F, Maffulli N. Small interfering RNAs in tendon homeostasis. *Br Med Bull*. 2021;138(1):58–67.
  9. Gargano G, Oliva F, Oliviero A, Maffulli N. Small interfering RNAs in the management of human rheumatoid arthritis. *Br Med Bull*. 2022;142(1):34–43.
  10. Gargano G, Asparago G, Spiezia F, Oliva F, Maffulli N. Small interfering RNAs in the management of human osteoporosis. *Br Med Bull*. 2023;148(1):58–69.
  11. Dong Z, Hu B, Wang S, Wang M, Sun S, Liu X, et al. LncRNA MAG12-AS3 promotes fracture healing through downregulation of miR-223-3p. *J Orthop Surg Res*. 2024;19(1):370.
  12. Selvakumar SC, Preethi KA, Sekar D. MicroRNAs as important players in regulating cancer through PTEN/PI3K/AKT signalling pathways. *Biochim Et Biophys Acta Reviews cancer*. 2023;1878(3):188904.
  13. Varshan MS, Selvakumar SC, Preethi KA, Murthykumar K, Ganapathy DM, Sekar D. MicroRNA-34a-3p and its target tumor necrosis factor- $\alpha$  in the regulation of South Indian oral squamous cell carcinoma population. *Minerva Dent Oral Sci*. 2024;73(5):256–63.
  14. Selvakumar SC, Preethi KA, Sekar D. MicroRNA-510-3p regulated vascular dysfunction in preeclampsia by targeting vascular endothelial growth factor A (VEGFA) and its signaling axis. *Placenta*. 2024;153:31–52.
  15. Yang A, Chen H, Lin J, Han M, Yuan X, Zhang T, et al. Comprehensive analysis of peripheral blood non-coding RNAs identifies a diagnostic panel for fungal infection after transplantation. *Bioengineered*. 2022;13(2):4039–50.
  16. Chen JW, Wang HJ, Zheng XF. [Research progress on mechanism of acupuncture and moxibustion promoting fracture healing]. *Zhongguo Gu Shang = China J Orthop Traumatol*. 2020;33(1):93–6.
  17. Luo J, Xiang H. LncRNA MYLK-AS1 acts as an oncogene by epigenetically silencing large tumor suppressor 2 (LATS2) in gastric cancer. *Bioengineered*. 2021;12(1):3101–12.
  18. Quan ZH, Xu FP, Huang Z, Chen RH, Xu QW, Lin L. LncRNA MYLK antisense RNA 1 activates cell division cycle 42/neutal Wiskott-Aldrich syndrome protein pathway via microRNA-101-5p to accelerate epithelial-to-mesenchymal transition of colon cancer cells. *Kaohsiung J Med Sci*. 2024;40(1):11–22.
  19. Zhu S, Zhang J, Gao X, Tang X, Cui Y, Li D, et al. Silencing of long noncoding RNA MYLK-AS1 suppresses nephroblastoma via down-regulation of CCNE1 through transcription factor TCF7L2. *J Cell Physiol*. 2021;236(8):5757–70.
  20. Zhang Y, Yuan Q, Wei Q, Li P, Zhuang Z, Li J, et al. Long noncoding RNA XIST modulates microRNA-135/CREB1 axis to influence osteogenic differentiation of osteoblast-like cells in mice with tibial fracture healing. *Hum Cell*. 2022;35(1):133–49.
  21. Waki T, Lee SY, Niihara T, Iwakura T, Dogaki Y, Okumachi E, et al. Profiling MicroRNA expression in fracture nonunions: potential role of MicroRNAs in nonunion formation studied in a rat model. *Bone Joint J*. 2015;97-b(8):1144–51.
  22. Ren Y, Wang S, Li H, Li J, Lan X, Wang Y. Low-energy red light-emitting diode irradiation enhances osteogenic differentiation of periodontal ligament stem cells by regulating miR-146a-5p. *J Periodontol Res*. 2024;59(5):1031–41.
  23. Peng N, Li J. Application effect of case management mode combined with ERAS in elderly patients with hip fracture. *Evidence-based complementary and alternative medicine*. eCAM. 2021;2021:1175020.
  24. Patel VS. Simultaneous bilateral femur neck fracture in A young adult with chronic renal Failure- A case report and review of literature. *J Orthop Case Rep*. 2015;5(4):24–6.
  25. Camarena V, Sant D, Mohseni M, Salerno T, Zaleski ML, Wang G, et al. Novel atherogenic pathways from the differential transcriptome analysis of diabetic epicardial adipose tissue. *Nutr Metab Cardiovasc Dis*. 2017;27(8):739–50.
  26. Zhai HY, Sui MH, Yu X, Qu Z, Hu JC, Sun HQ, et al. Overexpression of long Non-Coding RNA TUG1 promotes Colon cancer progression. *Med Sci Monit Int Med J Exp Clin Res*. 2016;22:3281–7.
  27. Kang R, Huang L, Zeng T, Ma J, Jin D. Long non-coding TRPM2-AS regulates fracture healing by targeting miR-545-3p/Bmp2. *J Orthop Surg Res*. 2024;19(1):466.
  28. Guo X, Zhang J, Han X, Wang G. LncRNA SNHG1 delayed fracture healing via modulating miR-181a-5p/PTEN Axis. *J Invest Surg*. 2022;35(6):1304–12.
  29. Lu Y, Gao Z, Liu C, Long M, Yang L, Li R, et al. Integrative analysis of lncRNA-miRNA-mRNA-associated competing endogenous RNA regulatory network involved in EV71 infection. *Am J Translational Res*. 2021;13(7):7440–57.
  30. Li G, Pan C, Sun J, Wan G, Sun J. LncRNA SOX2-OT regulates laryngeal cancer cell proliferation, migration and invasion and induces apoptosis by suppressing miR-654. *Experimental Therapeutic Med*. 2020;19(5):3316–24.
  31. Liu X, Zhou Z, Zeng WN, Zeng Q, Zhang X. The role of toll-like receptors in orchestrating osteogenic differentiation of mesenchymal stromal cells and osteoimmunology. *Front Cell Dev Biology*. 2023;11:1277686.
  32. Liu X, Zhang K, Wang L, Geng B, Liu Z, Yi Q, et al. Fluid shear stress-induced down-regulation of miR-146a-5p inhibits osteoblast apoptosis via targeting SMAD4. *Physiol Res*. 2022;71(6):835–48.
  33. Mangiavini L, Peretti GM, Canciani B, Maffulli N. Epidermal growth factor signalling pathway in endochondral ossification: an evidence-based narrative review. *Ann Med*. 2022;54(1):37–50.
  34. Gaii Via A, McCarthy MB, de Girolamo L, Ragni E, Oliva F, Maffulli N. Making them commit: strategies to influence phenotypic differentiation in mesenchymal stem cells. *Sports Med Arthrosc Rev*. 2018;26(2):64–9.
  35. Kay AG, Dale TP, Akram KM, Mohan P, Hampson K, Maffulli N, et al. BMP2 repression and optimized culture conditions promote human bone marrow-derived mesenchymal stem cell isolation. *Regen Med*. 2015;10(2):109–25.
  36. Barnaba S, Papalia R, Ruzzini L, Sgambato A, Maffulli N, Denaro V. Effect of pulsed electromagnetic fields on human osteoblast cultures. *Physiother Res Int*. 2013;18(2):109–14.
  37. Chen H, Xu C, Huang Q, Chen Y, Cheng K, Wang H, et al. Investigation of the impact of planar microelectrodes on macrophage-mediated mesenchymal stem cell osteogenesis. *Front Cell Dev Biology*. 2024;12:1401917.
  38. Deng F, Zhai W, Yin Y, Peng C, Ning C. Advanced protein adsorption properties of a novel silicate-based bioceramic: A proteomic analysis. *Bioactive Mater*. 2021;6(1):208–18.
  39. Cheng X, Zhao C. The correlation between serum levels of alkaline phosphatase and bone mineral density in adults aged 20 to 59 years. *Medicine*. 2023;102(32):e34755.
  40. Teng C, Tong Z, He Q, Zhu H, Wang L, Zhang X et al. Mesenchymal stem Cells-Hydrogel microspheres system for bone regeneration in calvarial defects. *Gels (Basel Switzerland)*. 2022;8(5).
  41. Salehi F, Dibaj M, Mohammadi A, Sattari M. Comparison of gene expression of different isoforms of osteopontin in symptomatic irreversible pulpitis of human dental pulp. *Iran Endodontic J*. 2022;17(1):1–6.
  42. Lee S, Kim M, Hong S, Kim EJ, Kim JH, Sohn Y, et al. Effects of sparganii rhizoma on osteoclast formation and osteoblast differentiation and on an OVX-Induced bone loss model. *Front Pharmacol*. 2021;12:797892.
  43. Mi M, Jin H, Wang B, Yukata K, Sheu TJ, Ke QH, et al. Chondrocyte BMP2 signaling plays an essential role in bone fracture healing. *Gene*. 2013;512(2):211–8.

## Publisher's note

Springer Nature remains neutral with regard to jurisdictional claims in published maps and institutional affiliations.